



European Commission
FP7, Grant Agreement 211743



Parametric instability of a cavity of Einstein Telescope

ET-xxx-09

Kazuhiro Yamamoto

Issue: 1

Date: September 6, 2009

Max-Planck-Institut für Gravitationsphysik (Albert-Einstein-Institut) and Universität Hannover
Callinstr. 38, 30167 Hannover, Germany

Contents

1	Introduction	1
2	Advanced LIGO and LCGT	2
2.1	Specifications of Advanced LIGO and LCGT	2
2.2	Parametric instabilities of Advanced LIGO and LCGT	2
2.3	Difference between Advanced LIGO and LCGT	3
2.3.1	Number of unstable modes	3
2.3.2	Mirror curvature dependence	3
2.3.3	Summary of discussion	3
3	Einstein Telescope	3
3.1	Specifications	3
3.2	Upper limit of R	4
3.3	Number of unstable modes	4
3.4	Mirror curvature dependence	5
4	Instability suppression	5
4.1	Thermal tuning method	5
4.2	Feedback control	5
4.3	Q reduction of elastic modes	5
5	Summary	6

1 Introduction

Parametric instability is one of the important issues in future interferometric detectors [1]. Such interferometers have at least a few km length arm cavities. The intervals of the optical modes in these long cavities are on the order of 10 kHz. This value is comparable with the intervals of elastic modes of mirrors of cavities. In such cases, the parametric instability becomes a serious problem in the stable operation of interferometers. Small thermally driven elastic vibration modulates the light and excites the transverse modes of the cavity. This excited optical modes apply modulated radiation pressure on the mirrors. This makes the amplitude of the elastic modes larger. At last, the elastic modes and optical modes, except for TEM00, oscillate largely. This is the parametric instability.

The formula of the parametric instability of a Fabry-Perot cavity (without anti-Stokes modes) is derived in Ref. [1]. If a parameter, R , of an elastic mode is larger than unity, that mode is unstable. The formula of R is

$$R = \sum_{\text{optical mode}} \frac{4PQ_mQ_o}{McL\omega_m^2} \frac{\Lambda_o}{1 + \Delta\omega^2/\delta_o^2}, \quad (1)$$

where $P, Q_m, Q_o, M, c, L, \omega_m, \Delta\omega$, and δ_o are the optical power in the cavity, the Q-values of the elastic and optical modes, the mass of the mirror, the speed of light, the cavity length, the angular frequency of the elastic mode, the angular frequency difference between the elastic and optical modes, and the half-width angular frequency of the optical mode, respectively. The value Λ_o represents the spatial overlap between the optical and elastic modes. If the shapes of the optical and elastic modes are similar, Λ_o is on the order of unity. If the shapes are not similar, Λ_o is almost zero. When the shapes and frequencies of the optical and elastic modes are similar ($\Lambda_o \sim 1, \Delta\omega \sim 0$), R will become several thousands in future projects. These parametric instabilities are a serious problem in Advanced LIGO [2, 3], one of the second generation interferometers. In another second generation detector, the LCGT interferometer, this instability is a less serious problem [4].

In this article, the parametric instability of the Einstein Telescope (ET) interferometer is discussed. This instability depends on the specification of the interferometer. However, details of the design are consider and

discussed now. Therefore, outlines of the instability of the ET interferometer and future work are shown. In order to simplify the discussion, only the instability of a Fabry-Perot cavity is considered. The effect of power and signal recycling (or resonant sideband extraction) techniques are not taken into account.

In Sec. 2, we consider the parametric instabilities in Advanced LIGO and LCGT as references. In Sec. 3, the parametric instability in ET is discussed. In Sec. 4, how to suppress the instability of the ET arm cavity is considered. Sec. 5 are devoted to a summary (and future work).

2 Advanced LIGO and LCGT

2.1 Specifications of Advanced LIGO and LCGT

Table 1 gives the specifications of Advanced LIGO in Refs. [2, 3, 5] (after these references, the specifications of Advanced LIGO were changed slightly) and LCGT [6] (the exact values of the LCGT mirror curvature are not fixed. The curvature given in Table 1 is only a candidate). The important differences between Advanced LIGO and LCGT are in the mirror curvature radius, beam radius, mirror material and temperature.

Table 1: Specification of Advanced LIGO [2, 3, 5] and LCGT [6].

	Advanced LIGO	LCGT
Laser beam profile	Gaussian	Gaussian
Wavelength(λ)	1064 nm	1064 nm
Cavity length(L)	4000 m	3000 m
Front mirror curvature radius(R_1)	2076 m	7114 m
End mirror curvature radius(R_2)	2076 m	7114 m
Beam radius at the mirrors(w_i)	60 mm	35 mm
Power in a cavity(P)	0.83 MW	0.41 MW
Mirror material	Fused silica	Sapphire
Mirror mass(M)	40 kg	30 kg
Mirror temperature(T)	300 K	20 K

2.2 Parametric instabilities of Advanced LIGO and LCGT

Study of the instability in Advanced LIGO by a group at the University of Western Australia [2, 3] is reviewed briefly. They investigated what happens when the curvature of a mirror is changed. The curvature of the other mirror is the default value given in Table 1. Reference [3] shows the curvature dependence of the unstable mode number. The number of the unstable modes of fused silica mirror cavity is between 20 and 60. Reference [2] shows that the maximum of R in the various elastic modes strongly depends on the mirror curvature. Even a shift of only a few meters in the mirror curvature causes a drastic change of the maximum R . The requirement of the accuracy in the mirror curvature in Advanced LIGO is difficult to be achieved.

A group of the University of Tokyo investigated the parametric instability of the LCGT arm cavity in the same manner as that of the University of Western Australia [4]. The number of the unstable modes is only $2 \sim 4$, which is 10-times smaller than that of Advanced LIGO. The mirror curvature dependence of the maximum R is weaker than that of Advanced LIGO. The maximum R is not changed drastically by a shift of a few meters in the mirror curvature. It is easier to satisfy the requirement of the mirror curvature in LCGT.

2.3 Difference between Advanced LIGO and LCGT

2.3.1 Number of unstable modes

The difference in the unstable mode numbers originates from the mode frequency density difference. If both of the optical and elastic mode densities are large, the optical mode frequencies often coincide with the elastic mode frequencies. The elastic mode density is inversely proportional to the cube of the sound velocity in the material. The sound velocities of the fused silica (Advanced LIGO) and sapphire (LCGT) are about 6 km/sec and 10 km/sec, respectively. The elastic mode density of LCGT is 5-times smaller. In Advanced LIGO, there are 7 optical transverse modes in a free spectrum range [2]. On the contrary, there are only 3 modes in the LCGT arm cavity. The optical mode density of LCGT is 2-times smaller. The larger optical mode density of Advanced LIGO stems from a larger beam radius to suppress the mirror thermal noise [7]. In LCGT, since the mirrors are cooled in order to reduce the thermal noise [6], larger beams are not necessary. As a result, the product of the elastic and optical mode densities of LCGT becomes 10-times smaller. As the results in Sec. 2.2, in actual, the unstable mode number calculated at the University of Tokyo for LCGT ($2 \sim 4$) is 10-times less than that calculated at the University of Western Australia for Advanced LIGO ($20 \sim 60$).

2.3.2 Mirror curvature dependence

In LCGT, the maximum value of R depends on the mirror curvature more weakly. This implies that the curvature dependence of the optical mode frequencies is weaker, because R is a function of the optical mode frequencies. The group of the University of Tokyo calculated how the curvature variation affects the n -th optical transverse mode [4]. The results are $15n$ Hz/m in Advanced LIGO and $0.58n$ Hz/m in LCGT. LCGT has a 30-times weaker curvature dependence due to the larger optical transversal mode spacing, which stems from the smaller beam radius.

2.3.3 Summary of discussion

The difference in the parametric instabilities between Advanced LIGO and LCGT is caused by those of the beam radii (Advanced LIGO, 60 mm; LCGT, 35 mm) and the mirror materials (Advanced LIGO, fused silica; LCGT, sapphire). These differences mostly originate from that of the thermal noise-reduction methods (Advanced LIGO, fused silica mirrors with larger laser beams; LCGT, cooling sapphire mirrors), which are the main strategies of the projects [4].

3 Einstein Telescope

3.1 Specifications

In this section, the parametric instability of the ET is considered. The details of the ET interferometer are not decided now. Here, we adopt parameters introduced by Stefan Hild [8]. These parameters are summarized in Table 2.

Hild supposed that the mass of a mirror M is 120 kg. It implies that the aspect ratio (the ratio of the mirror thickness to diameter) is smaller than those of usual interferometric gravitational wave detectors because of the large beam radius (12 cm). However, in order to simplify the discussion, it is assumed that the aspect ratio is the same as usual one (0.6 in LCGT). The mirror radius must be at least 2.5 times larger than the beam radius because the diffraction loss must be enough small¹. Thus, the mirror radius of ET is 30 cm. The mirror radius of LCGT is 12.5 cm. The volume of a mirror of ET is $(30/12.5)^3 = 2.4^3 = 14$ times larger than that of LCGT. The mirror mass of LCGT is about 30 kg. If the ET mirrors are made from sapphire as like LCGT, the mirror

¹In this case, the diffraction loss is 3.7 ppm.

Table 2: Specification of Advanced LIGO [2, 3, 5], LCGT [6] and ET [8].

	Advanced LIGO	LCGT	ET
Laser beam profile	Gaussian	Gaussian	Gaussian
Wavelength(λ)	1064 nm	1064 nm	1064 nm
Cavity length(L)	4000 m	3000 m	10000 m
Front mirror curvature radius(R_1)	2076 m	7114 m	5070 m
End mirror curvature radius(R_2)	2076 m	7114 m	5070 m
Beam radius at the mirrors(w_i)	60 mm	35 mm	120 mm
Power in a cavity(P)	0.83 MW	0.41 MW	3 MW
Mirror material	Fused silica	Sapphire	Silicon (or sapphire)
Mirror mass(M)	40 kg	30 kg	230 kg (or 410 kg)
Mirror temperature(T)	300 K	20 K	20 K

mass of ET is 410 kg. If the ET mirrors are made from silicon (densities of silicon and sapphire are 2.3 g/cm³ and 4 g/cm³), the mirror mass is 230 kg.

3.2 Upper limit of R

The upper limit of R is written as

$$R_{\text{upper}} = \frac{4PQ_m Q_o}{McL\omega_{m1}^2}, \quad (2)$$

where ω_{m1} is the angular resonant frequency of the fundamental elastic mode. Let us compare the upper limit of ET with that of LCGT. It is supposed that Q_m and Q_o of ET are as large as those of LCGT. Since the mirror of ET is 2.4 times larger than that of LCGT, the resonant frequency mirror ω_{m1} is 2.4 times smaller. If the ET mirrors are made from silicon, we must take the difference of the sound velocity into account (10 km/s in sapphire, 8.4 km/s in silicon). The resonant frequency ω_{m1} of silicon is 1.2 times smaller than that of a sapphire mirror with the same size. The upper limit of R of ET is 0.93 (sapphire) or 2.3 (silicon) times larger than that of LCGT.

3.3 Number of unstable modes

The mode density of the elastic mode is proportional to the cubic of the ratio of the mirror size to the sound velocity. If the ET mirrors are made from sapphire, the elastic mode density is 14 times larger than that of LCGT. If the ET mirrors are made from silicon, 23 times larger.

The ratio of the optical transverse mode interval to the free spectrum range is described as

$$\frac{1}{\pi} \cos^{-1} \sqrt{g_1 g_2}. \quad (3)$$

There are 3 and 13 transverse optical modes in a free spectrum range of LCGT and ET interferometers. Since the cavity of ET is 3 times longer, the free spectrum range is 3 times smaller. Therefore, the optical mode density of the ET interferometer is 14 times larger.

In total, the number of the instable modes, which is proportional to the product of the elastic and optical mode densities, of the ET interferometer is 190 (sapphire) or 310 (silicon) times larger than that of the LCGT interferometer. The reason why the number of the unstable modes in LCGT is 10 times less than that in Advanced LIGO is the cooled mirrors for the thermal noise reduction; sapphire mirrors and a normal beam size. Although the ET mirrors are cooled, the number of the unstable modes are larger. This is due to the larger beam radius and longer cavity length for the thermal noise reduction.

3.4 Mirror curvature dependence

The instability strength R is a function of the transverse optical mode frequencies. How the curvature variation affects the n -th optical transverse mode was calculated. The result is $4n$ Hz/m in ET. Since the beam radius of ET is larger, R of ET more strongly depends on the mirror curvature than that of LCGT ($0.58n$ Hz/m). Although the beam radius of ET is larger than that of Advanced LIGO, R more weakly depends on the mirror curvature ($15n$ Hz/m) because the cavity length is longer.

4 Instability suppression

Although the strength of the instability of the ET interferometer is comparable with that of advanced LIGO and LCGT, the number of the unstable modes is larger. The three methods for the instability suppression in Advanced LIGO are being studied [3, 9]. Let us consider whether these three methods (thermal tuning method, feedback control, Q reduction of elastic modes) are appropriate for ET (the tranquilizer cavity [10] is one of the other methods. However, this is difficult).

4.1 Thermal tuning method

In the thermal tuning method [3], a part of the mirror is heated for curvature control. Since R depends on the curvature, the suppression of R should be possible by this manner. However, this method is not useful in ET. Owing to the small thermal expansion and high thermal conductivity of cold sapphire and silicon, the mirror curvature would not change effectively, even if we apply heat to the mirror.

4.2 Feedback control

It is possible to control the light or the mirror so that the parametric instabilities would be actively suppressed [3]. If the number of unstable modes is smaller, feedback control is easier. However, these are more difficult (active) methods than Q reduction (passive method) of the elastic modes, especially, if there are many unstable modes.

4.3 Q reduction of elastic modes

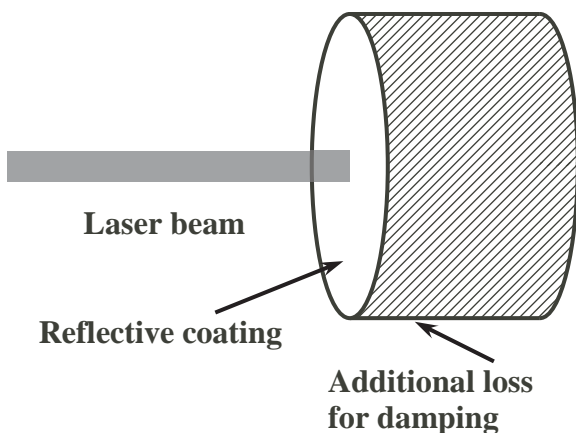


Figure 1: Loss on the barrel surface. Although this loss decreases the elastic Q-values of the mirror, Q_m , it has only a small contribution to the thermal noise [13, 14]. Thus, this loss suppresses the parametric instabilities without an increase of the thermal noise [9, 15].

This is a useful method [9] for ET. The value of R is proportional to the Q-value of the elastic mode, Q_m , as shown in Eq. (1). The Q-values of sapphire and silicon are about 10^8 [11, 12]. The maximum R of ET is

comparable with that of LCGT, several hundreds at most [4]. If the Q-values of the ET and LCGT mirrors become 10^6 , almost all modes become stable. Since the mechanical loss concentrated far from the beam spot has a small contribution to the thermal noise [13, 14], we should be able to apply additional loss on a barrel surface, as in Fig. 1, without sacrificing the thermal noise [9, 15]. The thermal noise of the barrel surface loss in LCGT is around $1.2 \times 10^{-24}/\sqrt{\text{Hz}}$ at 100 Hz in strain sensitivity. [4, 14, 16], when the LCGT mirror Q-values become 10^6 owing to the additional loss. As shown in Appendix A, the thermal noise by the barrel surface loss is inverse proportional to the square root of the mirror scale. Since the ET mirror is 2.4 times larger than that of LCGT in this article, the thermal noise is 1.5 times smaller in displacement sensitivity. The ET arm length is about 3.3 times longer than that of LCGT. The thermal noise of the barrel loss of the ET (sapphire) mirror in strain sensitivity is $2.3 \times 10^{-25}/\sqrt{\text{Hz}}$ at 100 Hz. This is comparable with the goal sensitivity of ET [8]. If the ET mirror is silicon, this thermal noise is $3.6 \times 10^{-25}/\sqrt{\text{Hz}}$ at 100 Hz because the thermal noise is inverse proportional to the square root of the Young's modulus of the mirror substrate. The detail is shown in Appendix B.

We are able to introduce the loss on the barrel surface by the coating Ta_2O_5 , which is a popular material for the reflective coating of the mirrors. According to Ref. [16], the loss angle of the $\text{SiO}_2/\text{Ta}_2\text{O}_5$ coating is $(4 \sim 6) \times 10^{-4}$ between 4 K and 300 K. Since the loss of this coating is dominated by that of Ta_2O_5 [17], the loss angle of Ta_2O_5 is $(8 \sim 12) \times 10^{-4}$. If the barrel loss dominates the mirror Q, it would be expressed as [14]

$$\frac{1}{Q_m} \sim \frac{E_{\text{Ta}_2\text{O}_5}}{E_{\text{substrate}}} \frac{2d}{R} \phi, \quad (4)$$

where $E_{\text{Ta}_2\text{O}_5}$, $E_{\text{substrate}}$, d , R , ϕ are the Young's moduli of Ta_2O_5 and the mirror substrate, the thickness of the Ta_2O_5 layer, the mirror radius, and the loss angle of Ta_2O_5 , respectively. These values are summarized in Table 3 [16, 18]. In order to make the Q-values, Q_m , 10^6 , the Ta_2O_5 coating thickness d must be 0.2 mm in the case of LCGT. Since the ET mirror is 2.4 times larger, d is 0.48 mm in the case of sapphire. If the substrate is silicon, d must be 0.2 mm.

Table 3: Specification of the coating [16, 18].

Young's modulus of the Ta_2O_5 ($E_{\text{Ta}_2\text{O}_5}$)	1.4×10^{11} Pa
Young's modulus of the sapphire	4.0×10^{11} Pa
Young's modulus of the silicon	1.64×10^{11} Pa
Mirror radius (R)	30 cm
Loss angle of Ta_2O_5 (ϕ)	10^{-3}

5 Summary

In this report, the parametric instability of a Fabry-Perot cavity in Einstein Telescope (ET) project was discussed. The maximum R is comparable with that in the second generation interferometers (Advanced LIGO and LCGT). Since the mirrors in LCGT will be cooled, the number of unstable modes of LCGT cavity is 10 times less than that of Advanced LIGO. The unstable mode number of ET is a few hundreds times larger than that of LCGT. Although the ET mirrors will be cooled, the larger beam radius and longer arm length increase the unstable mode number. The strength of instability R of ET depends on the mirror curvature more strongly than that of LCGT (because of the larger beam radius) and weakly than that of Advanced LIGO (because of the longer arm length). As like LCGT, the loss on the barrel surface is effective to suppress the parametric instability in ET. If there is 0.2 mm or 0.48 mm thickness Ta_2O_5 coating on the barrel surface of silicon or sapphire mirror, the parametric instability decreases sufficiently. The thermal noise caused by this loss on sapphire (or silicon) mirror is comparable with (or larger than) the goal sensitivity of ET.

Only the parametric instability of a Fabry Perot cavity in ET was considered in this report. We must investigate the instability of the total interferometer of ET and the instability suppression method based on details.

Appendix A : Mirror scale dependence of thermal noise by barrel surface loss

The ET mirror is larger than the LCGT mirror. We must consider the size effect on the thermal noise by the loss on the barrel surface. In order to simplify the discussion, it is supposed that the mirror and laser beam of ET are similar to those of LCGT. In short, the difference between ET and LCGT mirrors is only the scale. The ratio of beam radius to mirror radius is the same. Under this assumptions, Q-values of mirrors are independent of the mirror scale, a . According to Ref. [13], the amplitude of the thermal noise $\sqrt{G_{\text{coating}}}$ is described as

$$\sqrt{G_{\text{coating}}} \propto \sqrt{W_{\text{diss}}}, \quad (5)$$

where W_{diss} is the dissipated power when the pressure of which the profile $p(r)$ is the same as the laser beam is applied on the mirror flat surface. If the loss is the structure damping, the dissipated power is proportional to the elastic energy in the loss layer on the barrel surface;

$$W_{\text{diss}} \propto \int_{\text{barrel surface}} \mathcal{E} dS \times d, \quad (6)$$

where \mathcal{E} and d are the elastic energy density and the thickness of the loss layer. The problem is how W_{diss} depends on the mirror scale a . Since the mirrors are similar, dS and d are described as

$$dS \propto a^2, \quad (7)$$

$$d \propto a. \quad (8)$$

The elastic energy density \mathcal{E} is proportional to the square of the strain tensor. The strain tensor is proportional to the pressure on the flat surface p . This pressure is inverse proportional to the square of the scale. In short, the elastic energy density is written as

$$\mathcal{E} \propto p^2 \propto \frac{1}{a^4}. \quad (9)$$

We are able to obtain the relationship between the thermal noise and the mirror scale;

$$\sqrt{G_{\text{coating}}} \propto \sqrt{\frac{1}{a^4} \times a^2 \times a} = \sqrt{\frac{1}{a}}. \quad (10)$$

Above discussion is based on the assumption that the ratio of the beam radius to mirror radius is constant. If the mirror size is fixed, the barrel loss is independent of the beam size [14]. Therefore, the thermal noise by the barrel surface coating is inverse proportional to the square root of the mirror scale.

Appendix B : Mirror material dependence of thermal noise by barrel surface loss

Here we discuss how the thermal noise caused by the barrel surface loss depends on the material (Young's modulus) of the mirror substrate. It is supposed that the loss layer is made from Ta_2O_5 . Since the loss layer is thin, the strain in the loss layer is the same as that on the barrel surface of the mirror substrate. The strain tensor in the substrate is inverse proportional to the substrate Young's modulus $E_{\text{substrate}}$. The elastic energy density \mathcal{E} in the loss layer is proportional to the square of strain;

$$\mathcal{E} \propto \left(\frac{1}{E_{\text{substrate}}} \right)^2. \quad (11)$$

From Eqs. (5) and (6), the thermal noise of the barrel surface loss is derived;

$$\sqrt{G_{\text{coating}}} \propto \sqrt{\frac{d}{E_{\text{substrate}}^2}}. \quad (12)$$

We are able to rewrite this equation using Eq.(4);

$$\sqrt{G_{\text{coating}}} \propto \sqrt{\frac{1}{E_{\text{substrate}} Q_m}}. \quad (13)$$

Since Q_m must be about 10^6 , the thermal noise caused by the barrel surface loss is proportional to the square root of the Young's modulus of the mirror substrate.

References

- [1] V.B. Braginsky *et al.*, Phys. Lett. A **287** (2001) 331.
- [2] L. Ju *te al.*, Phys. Lett. A **354** (2006) 360.
- [3] L. Ju *te al.*, Phys. Lett. A **355** (2006) 419.
- [4] K. Yamamoto *et al.*, J. Phys.: Conf. Ser. **122** (2008) 012015.
- [5] C. Zhao *et al.*, Phys. Rev. Lett. **94** (2005) 121102.
- [6] K. Kuroda *et al.*, Prog. Theor. Phys. Suppl. **163** (2006) 54.
- [7] P. Fritschel, in *Proceedings of the SPIE meeting Gravitational-Wave Detection (4856-39), Waikoloa, Hawaii, 2002*, edited by P. Saulson and M. Cruise (International Society for Optical Engineering, Washington, 2002),p. 282.
- [8] S. Hild *et al.*, arXiv:0810.0604. Now, this sensitivity is called ET-B.
- [9] S. Gras S *et al.*, J. Phys.: Conf. Ser. **32** (2006) 251.
- [10] V.B. Braginsky *et al.*, Phys. Lett. A **293** (2002) 228.
- [11] T. Uchiyama *et al.*, Phys. Lett. A **261** (1999) 5.
- [12] R. Nawrodt *et al.*, J. Phys.: Conf. Ser. **122** (2008) 012008.
- [13] Y. Levin, Phys. Rev. D **57** (1998) 659.
- [14] K. Yamamoto *et al.*, Phys. Lett. A **305** (2002) 18.
- [15] S. Gras *et al.*, Phys. Lett. A **333** (2004) 1.
- [16] K. Yamamoto *et al.*, Phys. Rev. D **74** (2006) 022002.
- [17] S.D. Penn *et al.*, Class. Quantum Grav. **20** (2003) 2917.
- [18] S. Hild *et al.*, arXiv:0906.2655.

1

1, 2, 3, 4

1, 2, 4, 5

1, 2, 3, 6

2, 4

2, 3, 4

3

3, 4, 6

5, 6

5

5

5

5, 6

5, 6, 7

5, 6

6

6

6